
Article:
Mann, C. orcid.org/0000-0002-8781-1652, Eskelsen, J.R., Leonard, D.N. et al. (2 more authors) (2020) The dissolution of simulant vitrified intermediate level nuclear waste in young cement water. MRS Advances, 5 (3-4). pp. 131-140. ISSN 2059-8521

https://doi.org/10.1557/adv.2020.40

MRS Advances

The dissolution of simulant vitrified intermediate level nuclear waste in young cement water

Colleen Mann,[1] Jeremy R. Eskelsen[2], Donovan N. Leonard[2] Eric Pierce[2] and Claire L Corkhill[1]

[1]*Immobilisation Science Laboratory, Department of Materials Science and Engineering, The University of Sheffield, Sir Robert Hadfield Building, Mappin Street, Sheffield S1 3JD, UK*

[2]*Oak Ridge National Laboratory, Oak Ridge, TN, USA*

It is pertinent to the safety case for geological disposal in the UK that the behaviour of vitrified wastes in proximity to cementitious materials is understood. In this study, vitrified simulant intermediate level nuclear waste (ILW) was subject to dissolution in a synthetic cement water solution to simulate disposal conditions. Results show that the presence of alkali / alkaline earth elements in the cementitious solution can be favourable, at least in the short-term, leading to lower dissolution rates associated with incorporation of these elements into the altered layer of the glass.

Corresponding author. Email address: c.corkhill@sheffield.ac.uk (C L Corkhill)

INTRODUCTION

In recent years, the effects of disposing of vitrified nuclear waste in high pH, cement rich environments have been investigated; in particular, the UK and Belgium are considering geological disposal scenarios where glass will be in close proximity to cementitious materials. In the UK, the possibility for co-disposal of vitrified intermediate level waste (ILW) with cementitious ILW is being explored; if this is in a hard-rock geology (e.g. granite), a Portland cement / limestone blend material, known as Nirex Reference Vault Backfill (NRVB) [1], may be employed as a backfill. It is therefore necessary to undertake performance assessments to determine the compatibility of vitrified ILW and NRVB [1].

Portland cement is composed of Ca-silicates, Ca-aluminate, Ca-Al-ferrite and other minor components including Ca-sulphates, calcite, Mg-hydroxide and Na/K

sulphates[2]. Within a geological disposal facility (GDF), when Portland cement comes into contact with groundwater, K and Na will be the first elements to leach from the cement in the form of hydroxides, giving rise to solutions with high pH (pH $\geq$ 13). With continual replenishment of groundwater, the cement hydrate phase, portlandite $Ca(OH)_2$, will be leached, resulting in a pH of 12. Once the Ca is depleted from portlandite, calcium silicate hydrate (C-S-H) phases will be dissolved, reducing the pH of the groundwater to between 10 and 11 [2][3].

Under such hyperalkaline conditions, the solubility of Si, Al and Zr from the glass matrix increases [2][5][6] and, when alkali and alkaline earth elements released from the cement interact with the silica gel, it can influence the overall glass dissolution rate [6]–[8]. In this study, we investigate the nature of cement water solution – silica gel interaction at the surface of a simulant ILW glass, and the subsequent effect on the dissolution rate, providing microscopic analysis of the surface layers formed on the glass by Scanning Electron Microscopy (SEM) and Transmission Electron Microscopy (TEM).

METHODOLOGY

Glass synthesis

The Laboratory BoroSilicate glass (LBS) was developed at the University of Sheffield as a demonstration of the feasibility to immobilise a typical ILW Magnox waste stream [9][10]. This alkali borosilicate glass has a 30 wt% loading of the simulant ILW waste stream, comprising; 20 wt% $Mg(OH)_2$, 30 wt% clinoptilolite ion exchange resin, 30 wt% sulphonic ion exchange resin and 20 wt% radionuclide surrogates (Cs_2O, SrO, CeO_2, La_2O_3) in addition to metallic corrosion products (Fe_2O_3, Al_2O_3, ZrO_2) [9][10].

The oxide precursors for the LBS glass were weighed and mixed prior to the melt. The melt was fluid at 1000 ºC. The analysed composition is detailed in Table I. The oxide precursors were; $Al(OH)_3$ (>99.9 % Acros), H_3BO_3 (>99.9 % Merck), $BaCO_3$ (99% Alfa Aeser), $CaCO_3$ (96% Fluka), CeO_2 (99.5% Alfa Aesar), $CsCO_3$ (99% FluroChem), Fe_2O_3 (98% Alfa Aesar), K_2CO_3 (99% Sigma), La_2CO_3 (99% Testbourne), $LiCO_3$ (99.5% Analar), MgO (99.9% Acros), MoO_3 (99% Sigma), Na_2CO_3 (98% Alfa Aesar), SiO_2 (95%), $SrCO_3$ (99.9% Sigma) and ZrO_2 (99 % Aldrich). For additional details on melt conditions see Utton et al. [11].

Table I. LBS glass composition, as determined by ICP-OES analysis after total acid digest.

	wt%		wt%
SiO_2	47.92 ± 2.4	**La_2O_3**	1.53 ± 0.08
B_2O_3	9.62 ± 0.48	**SrO**	0.13 ± 0.01
Na_2O	12.94 ± 0.65	**NiO**	0.05 ± 0.001
Li_2O	3.9 ± 0.2	**CaO**	0.45 ± 0.02
ZrO_2	0.67 ± 0.03	**K_2O**	0.15 ± 0.01
MoO_3	0.52 ± 0.03	**Cr_2O_3**	0.01 ± 0.001
Al_2O_3	6.85 ± 0.34	**SO_3**	0.02 ± 0.001
Fe_2O_3	10.25 ± 0.51	**TiO_2**	0.01 ± 0.001
Cs_2O	0.69 ± 0.03	**Cu_2O**	0.02 ± 0.001
MgO	3.71 ± 0.19	**ZnO**	0.01 ± 0.001
CeO_2	0.36 ± 0.02		
BaO	0.11 ± 0.01	**Total**	**99.95**

Dissolution methodology

A solution of "young cement water with added calcium" (YCWCa), was designed to simulate the composition of the initial leachate formed when groundwater contacts Portland cement, was prepared under anaerobic conditions according to the composition of Ferrand et al. [12] (Table II).

Table II Composition of synthetic young cement water with added calcium (YCWCa), in mmol L^{-1}. The pH of the resulting solution is pH (RT)13.0 ±0.4.

	Ca	Na	K	Al	Si	S	C
YCWCa	0.46 ± 0.1	68.68 ± 4.09	353 ± 19	0.00 ±0.00	0.25 ± 0.17	2.18 ± 0.06	0.30 ± 0.06

Dissolution experiments were performed according to the ASTM PCT-B methodology [13] at 50°C for 112 days, under CO_2-free conditions, to avoid carbonation of the solution. Glass was ground to a particle size of 75–150 µm prior to washing, according to the PCT-B standard. The surface area to volume ratio utilised was 1200 m^{-1}. Experiments were performed in triplicate with duplicate blanks, sacrificial sampling took place on days 1, 3, 7, 14, 21, 28, 56, 64, 72, 84 and 112. Aliquots of solution were taken for pH measurements and elemental concentration analysis by Inductively Coupled Plasma-Optical Emission Spectroscopy (ICP-OES, ThermoFisher iCAPduo6300), utilising a ceramic torch and internal standard. The normalised mass loss NL (g m^{-2}) of each element, i, in solution was calculated using Equation 1, where C_i is the concentration of element i in solution g m^{-3}, $C_{i,b}$ is the concentration of element i in the blank solution (g m^{-3}), f_i is the mass fraction of element i in the glass and SA/V is the surface area to volume ratio (m^{-1}), corrected for evaporative loss.

$$NL_i = (C_i - C_{i,b}) / \left(f_i \times \frac{SA}{V}\right) \quad (1)$$

The normalised dissolution rate (NR, g m^{-2} d^{-1}) was calculated using a linear fit of the NL_B; NR_0 relates to the dissolution rate prior to the transition to the "affinity controlled" dissolution regime (measured between 1 – 7 d), while NR_a relates to the "affinity controlled" dissolution rate, where the dissolution rate slows due to the build-up of soluble species from the glass into the solution (measured between 14-84 days), which can lead to the formation of alteration products on the surface of the glass.

Alteration Layer Analysis

At each sampling point, the glass was removed from the solution and left to dry at room temperature overnight, prior to encapsulation in epoxy resin for analysis by Scanning Electron Microscopy (Hitachi TM3030 Plus, operating at an accelerating voltage of 5 kV, and Inspect F50 SEM operating at an accelerating voltage of 15 kV). Both microscopes were coupled with an Energy Dispersive Electron Spectroscopy detector. Both secondary electron and backscattered electron images were taken to provide both topographical and elemental information about the alteration products that formed on the surface of glass grains.

Focused ion beam (FIB) lift-outs were taken from the glass samples (FIB-SEM Hitachi NB5000). The lift-out targeted the boundary between pristine glass and the alteration products. Analysis of the FIB samples was performed by Transmission Electron Microscopy (TEM), using a cold field emission Hitachi HF-3300 high resolution TEM with the capabilities of STEM and SEM with an accelerating voltage of 300 kV. EDS was performed using a Bruker XFlash silicon drift detector.

X-ray diffraction (XRD) data were acquired in 2θ reflection mode on a Bruker D2 Phaser X-ray diffractometer, with Cu Kα radiation, using a Ni filter and Lynx-Eye position sensitive knife edge (1 mm) to eliminate stray scatter. The acquisition parameters were: Start 2θ = 5°, end 2θ = 70°, step size = 0.02° effective total scan time = 3 hours, sample rotation = 60 Hz, Lynx-Eye Detector settings were: lower discriminator = 0.110, upper discriminator = 0.250. The X-ray tube settings were 30 kV and 10 mA.

Geochemical Modelling

Geochemical modelling was performed using PhreeqC version 3, utilising the ThermoChimie PhreeqC Davies electron v10a database [14]. The concentrations of elements measured by ICP-OES, in addition to measured pH values, were input into the software to calculate the saturation indices of phases present in the database.

RESULTS AND DISCUSSION

The average concentration of K in solutions contacted with glass powders was similar to that observed in the blank (~9000 ± 500 mg L^{-1}), the concentration remained fairly consistent throughout the duration of the experiment. It is likely that there was a rapid uptake of K from the solution by the glass, as observed in previous investigations of

the International Simple Glass in young cement solutions [7]. The pH also remained constant, at pH(RT) 13.02 ± 0.4, in samples and blank solutions.

The normalised mass loss of elements from the glass to solution is shown in Figure 1. After an initial rapid release of B (NR_0 = (20.6 ± 0.4) x 10^{-2} g m^{-2} d^{-1}), the NL_B continued to increase throughout the experiment, in a nearly linear fashion (NR_a = (4.42 ± 0.2) x 10^{-2} g m^{-2} d^{-1}), until the last time point when it increased significantly (Figure 1a). The NL_{Li}, NL_{Si} and NL_{Mg} followed a similar trend (Figures 1b-e), although the absolute value of the NL_{Mg} was significantly lower than the other elements. Furthermore, the NL_{Na} exhibited a plateau between 56 and 84 d. The NL_{Al} increased until 14 d, at which point it continually decreased.

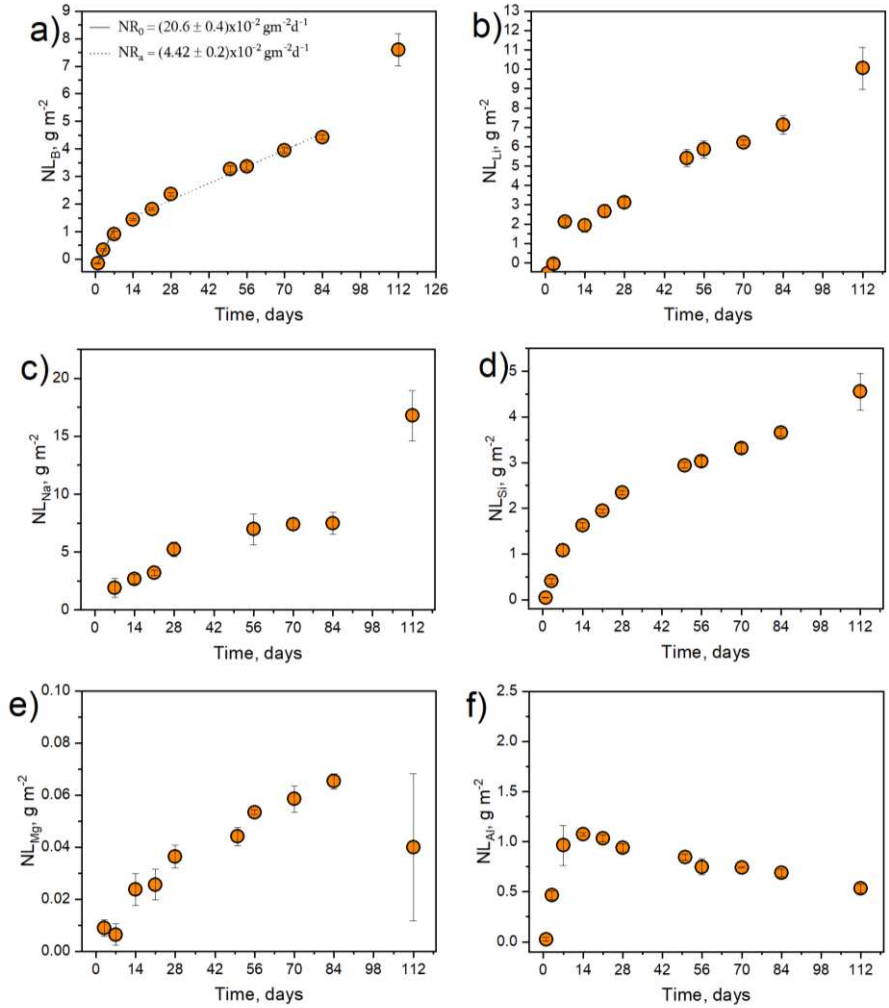

Figure 1 Normalised mass loss of elements from the LBS glass into YCWCa solution over 112 days. The error was determined by the standard deviation of triplicate measurements.

Alteration products were observed on the surfaces of the glass grains. Figure 2a shows SEM images of the altered layer, comprising of an amorphous gel layer and secondary phases, formed after 7, 21, 56 and 84 days; Figure 2b details how the thickness of the altered layer changed as a function of dissolution time. The most significant growth in the alteration layer took place between day 56 and 84 when the layer almost doubled in thickness.

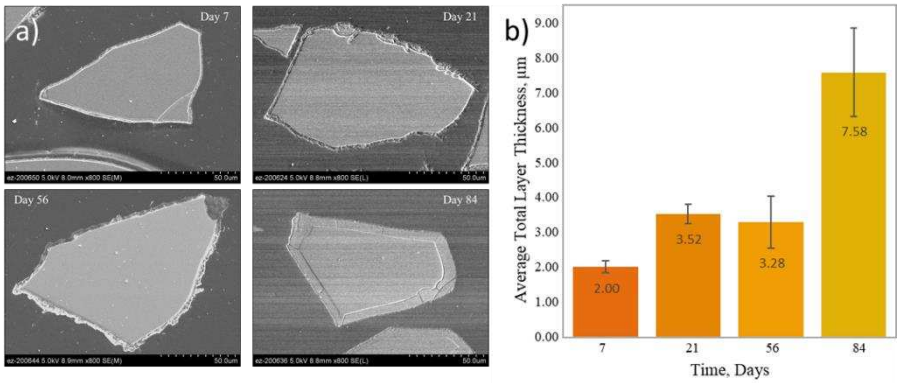

Figure 2 (a) SE-SEM images of glass grains at 7, 21, 56 and 84 days; and (b) average alteration layer thickness as measured by >280 line measurements on 7 SEM images of glass grains.

Elemental analysis of the alteration layer using SEM-EDX (Figure 3) showed that in comparison to the bulk glass, there was an elevated concentration of K. Combined with slight decrease in K concentration in solution, this confirms that K was taken into the glass alteration layer. In accordance with studies of other glass compositions in YCWCa solution [7][12], it is apparent that this layer is a K-rich alkali silica gel. The outer edge of the alteration layer appeared to be composed of fine particles (<1 µm in size), and was found to be enriched in Ca. Analysis of the glass powders by X-ray diffraction (data not shown) did not reveal the presence of any crystalline mineral phases other than portlandite ($CaOH_2$). The bright spots in the back scattered image were found to contain Fe in addition to Ca.

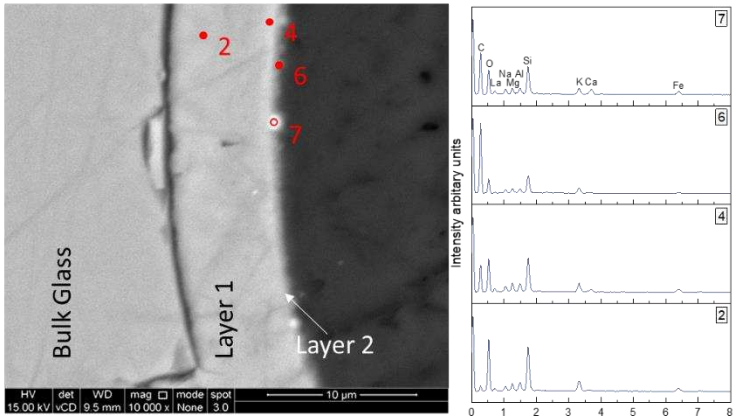

Element	Na	Mg	Al	Si	S	K	Ca	Fe	Other
Avg at% Bulk glass	21.95 ± 1.06	6.36 ± 0.32	8.03 ± 0.36	54.46 ± 2.71	-	0.19 ± 0.02	0.33 ± 0.03	7.74 ± 0.46	0.46 ± 0.05
Avg at% Layer 1 (2)	7.22 ± 0.27	8.30 ± 0.15	8.65 ± 0.19	46.18 ± 0.10	-	15.16 ± 0.28	-	12.19 ± 0.11	0.62 ± 0.15
Avg at% Layer 2 (4)	9.73 ± 0.78	10.45 ± 0.63	8.92 ± 0.15	38.29 ± 0.86	-	14.06 ± 2.05	3.26 ± 2.15	14.11 ± 0.50	0.60 ± 0.16
at% Spot 6	11.52 ± 0.58	9.79 ± 0.49	8.45 ± 0.42	36.30 ± 1.82	2.69 ± 0.13	16.04 ± 0.80	-	-	0.58 ± 0.57
at % Spot 7	10.21 ± 0.51	8.18 ± 0.41	6.94 ± 0.35	36.30 ± 1.82	0.00 ± 0.00	10.62 ± 0.53	11.14 ± 0.56	-	0.51 ± 0.31

Figure 3 BSE-SEM-EDX analysis of a LBS grain exposed to YCWCa for 84 days. The spectra correspond to spot analysis at the points indicated on the image. The table provides an average at% based on three spots taken in each region apart from spot 7 which is an isolated feature.

A Focussed Ion Beam (FIB) sample was taken from the altered region of a grain of LBS glass for analysis by Transmission Electron Microscopy (TEM). The grain selected exhibited an alteration layer of 1.23 ± 0.8 µm. Bright field images of the altered layer, shown in Figure 4a, in conjunction with EDX analysis, showed that the boundary between the bulk glass and the "gel layer" was not sharp, but nonetheless distinct. Several zones could be identified, as shown in Figure 4a: (i) the gel layer had a higher Z contrast than the bulk glass, was 1.05 ± 0.8 µm thick, and had elevated concentrations of K and Na in comparison to the bulk glass; (ii) a very high Z contrast layer ~ 60 nm resided on the outer edge of the gel layer and contained Ca-bearing nodule-like features; and (iii) the outer layer was rich in Mg and was comprised of needle-like precipitate phases, similar in morphology to amorphous phases known to be precursors to the nucleation of clay minerals, such as saponite ($Ca_{0.25}(Mg,Fe)_3((Si,Al)_4O_{10})(OH)_2 \cdot n(H_2O)$). These phases have previously been identified to develop into clay minerals at the surface of simulant nuclear waste glasses dissolved at 90°C [15]. PhreeqC modelling of the system predicted that the phyllosilicate minerals; saponite-K/Mg/Na and phlogopite-K/Na ($KMg_3(AlSi_3O_{10})(OH)_2$), and Mg bearing phases; brucite ($Mg(OH)_2$) and hydrotalcite ($Mg_4Al_2(OH)_{14}.3H_2O$), should be saturated in solution after 21 days. Phillipsite-K ($K(Si,Al)_8O_{16}.6H_2O$) was also predicted to be saturated between day 35-112.

Selected area electron diffraction (SAED) performed within each of the different regions of the FIB section, including the needle-like ribbons, resulted in the collection of amorphous diffraction patterns, indicating the non-crystalline nature of the altered layer; damage to these materials through the interaction of the electron beam, however, cannot be ruled out. It was possible to identify the composition of the nodule as calcite ($CaCO_3$) (Figure 4b and d).

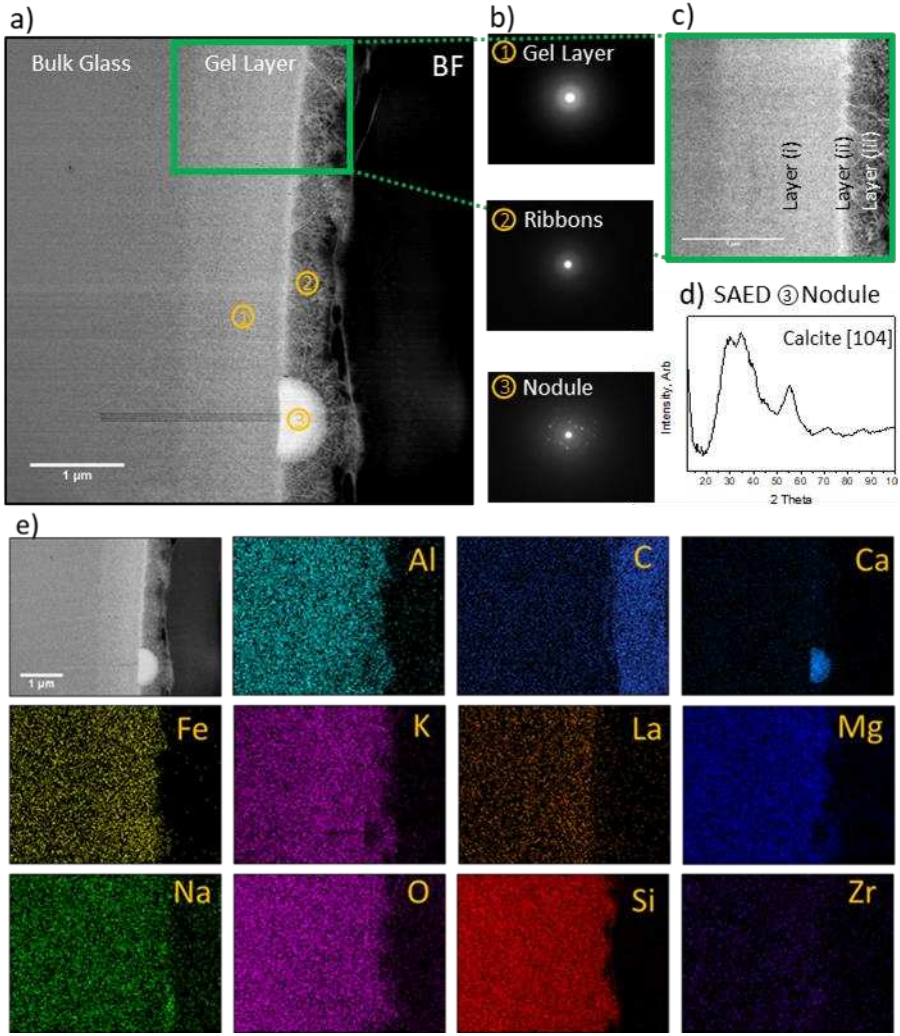

Figure 4 a) TEM bright field (BF) images of the alteration regions on LBS glass exposed to YCWCa for 84 days. b) SAED patterns of the spots shown on the BF image, depicted by the numbered circles, c) is a magnified region highlighted by the green box, identifying three distinct alteration layers on the surface of the glass, d) SAED is shown of the nodule.

CONCLUSION

An investigation of the effect of the complex geochemical conditions of a cementitious geological disposal facility on glass alteration was performed. Our findings show that the interaction of elements from the cement solution, particularly K, with the glass give rise to the formation of an amorphous alkali-silica gel. TEM analysis identified three distinct alteration layers residing on the surface of the glass, with the outer most layer (needle-like precipitates/ribbons) possibly comprising clay minerals. The initial dissolution rate obtained in this study (0.062 ± 0.007 $gm^{-2}d^{-1}$), is comparable to that of Utton's where LBS glass was dissolved in pure water (0.05 ± 0.001 $gm^{-2}d^{-1}$ at 50 ^{o}C [16]),

this suggests that the presence of cement water in a geological disposal facility may not be detrimental to the durability of the glass, assuming that the high initial rate is hindered by the development of a Si-rich gel layer.

ACKNOWLEDGEMENTS

The UK research team are grateful to the Engineering and Physical Science Research Council for funding under grant awards EP/N017374/1, EP/G037140/1 and we wish to acknowledge the Henry Royce Institute for Advanced Materials (EPSRC award EP/R00661X/1) for the financial support and equipment access at Royce@Sheffield. This research was performed, in part, at the MIDAS Facility, at the University of Sheffield, which was established with support from the Department of Energy and Climate Change. The portions of the research conducted at Oak Ridge National Laboratory (ORNL) were supported by the US Department of Energy's Office of Environmental Management (EM) Tank Waste Management program. ORNL is operated by UT-Battelle, LLC for the US DOE under Contract No. DE-AC05-00OR22725.

References

[1] R. G. W. Vasconcelos, N. Beaudoin, A. Hamilton, N. C. Hyatt, J. L. Provis, and C. L. Corkhill, 'Characterisation of a high pH cement backfill for the geological disposal of nuclear waste: The Nirex Reference Vault Backfill', *Appl. Geochemistry*, vol. 89, no. July 2017, pp. 180–189, 2018.

[2] B. Lothenbach, G. Le Saout, E. Gallucci, and K. Scrivener, 'Influence of limestone on the hydration of Portland cements', Cement and Concrete Research, Jun. 2008.

[3] C. dit Coumes, *Low pH cements for waste repositories: A review*. 2008.

[4] S. Ribet and S. Gin, 'Role of neoformed phases on the mechanisms controlling the resumption of SON68 glass alteration in alkaline media', *J. Nucl. Mater.*, vol. 324, no. 2–3, pp. 152–164, 2004.

[5] S. Mercado-Depierre, F. Angeli, F. Frizon, and S. Gin, 'Antagonist effects of calcium on borosilicate glass alteration', *J. Nucl. Mater.*, vol. 441, no. 1–3, pp. 402–410, Oct. 2013.

[6] S. Gin *et al.*, 'The fate of silicon during glass corrosion under alkaline conditions: A mechanistic and kinetic study with the International Simple Glass', *Geochim. Cosmochim. Acta*, vol. 151, pp. 68–85, 2015.

[7] C. Mann *et al.*, 'Influence of young cement water on the corrosion of the International Simple Glass', *npj Mater. Degrad.*, vol. 3, no. 1, pp. 1–9, 2019.

[8] C. L. Corkhill, N. J. Cassingham, P. G. Heath, and N. C. Hyatt, 'Dissolution of UK High-Level Waste Glass Under Simulated Hyperalkaline Conditions of a Colocated Geological Disposal Facility', *Int. J. Appl. Glas. Sci.*, vol. 4, no. 4, pp. 341–356, Dec. 2013.

[9] C. A. Utton, R. J. Hand, P. A. Bingham, N. C. Hyatt, S. W. Swanton, and S. J. Williams, 'Dissolution of vitrified wastes in a high-pH calcium-rich solution', *J. Nucl. Mater.*, vol. 435, no. 1–3, pp. 112–122, 2013.

[10] C. A. Utton, N. C. Hyatt, and S. W. Swanton, 'Interactions of vitrified wastes with NRVB A report to NDA RWMD', 2012.

[11] C. A. Utton, R. J. Hand, N. C. Hyatt, S. W. Swanton, and S. J. Williams, 'Formation of alteration products during dissolution of vitrified ILW in a high-pH calcium-rich solution', Journal of Nuclear Materials, 2013.

[12] K. Ferrand, S. Liu, and K. Lemmens, 'The Interaction Between Nuclear Waste Glass and Ordinary Portland Cement', *Int. J. Appl. Glas. Sci.*, vol. 4, no. 4, pp. 328–340, Dec. 2013.

[13] A. Int'l, 'Standard Test Methods for Determining Chemical Durability of Nuclear , Hazardous , and Mixed Waste Glasses and Multiphase Glass Ceramics : The Product Consistency Test (PCT) 1'.

[14] E. Giffaut *et al.*, 'Andra thermodynamic database for performance assessment: ThermoChimie', *Appl. Geochemistry*, vol. 49, pp. 225–236, 2014.

[15] T. A. Abrajano, J. K. Bates, A. B. Woodi-and, and W. L. Bourcier, 'Secondary phase formation during nuclear waste-glass dissolution', *Clays Clay Miner.*, vol. 38, no. 5, pp. 537–548, 1990.

[16] J. M. Schofield *et al.*, 'Experimental studies of the chemical durability of UK HLW and ILW glasses. First interim progress report (RWM005105)', 2013.